J. Electrochem. Sci. Eng. **12(3)** (2022) 511-527; http://dx.doi.org/10.5599/jese.1220

Open Access : : ISSN 1847-9286

https://pub.iapchem.org/ojs/index.php/JESE

Original scientific paper

Simulation of corrosion protection methods in reinforced concrete by artificial neural networks and fuzzy logic

Alireza Afshar[1], Ali Shokrgozar[2,✉], Abdollah Afshar[3] and Amirhossein Afshar[4]

[1]*Department of Civil and Environmental Engineering, George Mason University, Fairfax, VA, USA*
[2]*Department of Civil and Environmental Engineering, Idaho State University, 921 S 8th Ave, Mail Stop 8060, Pocatello, Idaho, 83209 USA*
[3]*Department of Materials Science and Engineering, Sharif University of Technology, Tehran, Iran*
[4]*Department of Civil and Environmental Engineering, Sharif University of Technology, Tehran, Iran*

Corresponding author: ✉ shokali@isu.edu; Tel:+1208252 8792

Received: December 12, 2021; Accepted: February 17, 2022; Published: April 1, 2022

Abstract

In this study, the effect of protection methods regarding the corrosion decrement of steel in concrete was simulated by artificial neural networks (ANNs) and fuzzy logic (FL) approaches. Hot dip galvanizing as a protective coating, Ferrogard 901 corrosion inhibitor, a pozzolanic component, such as fly ash (FA) and micro-silica (MS), and eventually rebar AISI-304 were employed in concrete. Reinforced concrete samples were held under impressed voltage of 30 V in 3.5 % NaCl electrolyte for 350 hours toward a stainless-steel auxiliary electrode. Corrosion currents have been modelled using feed forward back propagation ANNs and FL methods. The results demonstrate good consistency between corrosion data and simulated models. Furthermore, the correlation coefficient criterion clearly indicates using pozzolanic materials, with a combination of MS and FA, can be introduced as one of the best corrosion protection methods, with a 35 % contribution factor in reinforced concrete.

Keywords

Simulation, corrosion, concrete, neural networks, fuzzy logic

Introduction

Ingress of water and aggressive fluids is the main reason responsible for major chemical and physical degradation of concrete pavements and structures, which decreases their durability and life span [1-11]. Reinforced concrete has a great significance in the durability and stability of marine structures [12]. The premature deterioration of concrete buildings and infrastructure due to reinforcement corrosion is a severe challenge, both technically and economically [13,14]. Reinforcement corrosion owing to passive layer disruption, γ-$Fe_2O_3 \times H_2O$, accompanying chloride ion diffusion ones through concrete is started. Different methods have been suggested to reduce the corrosion rate of steel reinforcements in concrete. The most important methods include pozzolanic additives, *i.e.,* micro silica (MS) [15], fly ash

(FA) [16,17] and granulated blast furnace slag [18], to prepare very dense and strong types of concrete, rebar or concrete coating [19-21], the alteration of the steel alloy composition [22], and corrosion inhibitor admixtures [23]. Today, the combination of artificial neural networks (ANNs) and fuzzy logic (FL) methods as powerful tools to analyze and simulate phenomena are used to predict concrete features, such as compression strength. Moreover, the ability to work with incomplete knowledge, prediction of reinforced concrete parameters, and having fault tolerance are some of the advantages of using these methods [24-33]. It is worth recalling that there are restricted studies on the simulation of the corrosion current of the rebar or the degradation of reinforced concrete by ANNs and FL. In this regard, Topcu and coworkers have modeled both the compressive strength and the corrosion current of steel in concrete by ANNs regarding the addition of fly ash to the concrete mix design [34]. In another study, Ukrainczyk and coworker have analyzed the relationships between numerous input parameters and observed damage owing to reinforcement corrosion with ANNs and the fuzzy prediction [35]. Parthiban *et al.* have simulated the corrosion of steel in concrete through potential monitoring in accordance with ASTM C876 for a long time only by ANNs [36].

This study attempts to evaluate the influence of different protection methods on the enhancement of corrosion resistance of reinforced concrete by ANNs and FL approaches. These protection methods were applied by replacing stainless steel (AISI 304) with carbon steel rebar, coating carbon steel reinforcement by the hot dip galvanized film, the addition of pozzolanic materials, such as the MS and FA in the optimum content of 10 and 25 wt.% of cement, respectively, in concrete [37,38], and finally, the addition of the corrosion inhibitor admixture, Ferrogard 901, to the concrete mixing design. In this research, the effects of the aforementioned parameters on the corrosion behavior of reinforcement and its durability in the simulated seawater solution (3.5 % NaCl) [39] have been predicted by ANNs and FL and compared to the actual results of the accelerated corrosion test. AISI-304 rebar, hot dipping galvanized coating, accelerated corrosion test, and FL method are the parameters that have not been studied in the previous research. In all cases, the accelerated corrosion current at an impressed anodic potential of 32 V, applied between the stainless-steel counter electrode and the working electrode (rebar), was monitored at each 30 min interval by the designed data logger. Eventually, the nonlinear response of the galvanic current, as well as the performance of each protective method to enhance the corrosion resistance of the reinforcement, was evaluated. The simulated results are in good consistency with the experimental ones.

Experimental

Materials

In the experiments, Tehran cement type II represented in Table 1, double washed sand in the range of 4.5 to 9 mm, river sand, Ferrogard 901 as a corrosion inhibitor admixture (Table 2), carbon steel, A-20 grade, and stainless steel, AISI-304 grade, as reinforcements (Table 3) and 3.5 wt.% NaCl solution for electrochemical tests was employed. Besides, MS and FA, as shown in Table 1, in the optimum content of 10 and 25 wt.% cement regarding the improvement of concrete properties were added to the mix design, respectively [40].

Concrete mix design

Three types of concrete (Table. 4) were prepared, which in the mixing patterns of A and B, controlling samples accompanied with concrete concerning corrosion inhibitor admixture with a w/c of 0.4 were presented. Furthermore, in the third mixing design, the simultaneous effect of FA and MS at a percent of 25 and 10 wt.% cement was utilized, respectively.

Table 1. *Chemical composition of cement type II, FA and MS*

	Cement type II	FA	MS
	Content, wt.%		
CaO	62	4.62	3
SiO_2	21	51.5	94
Al_2O_3	3.3	30.5	0.4
Fe_2O_3	1.5	6.7	0.7
MgO	5.5	3	0.1
SO_3	1.7	0.4	0.15
Na_2O	0.14	0.43	0.23
K_2O	0.64	0.55	0.44
Cl	0.012	0.007	0.002
Loss of ignition	7.13	2.17	2.87
Free lime	1.84	0.14	0.11
Specific gravity	2.96	2.78	1.98

Table 2. *Inhibitor admixture specification*

Production name	Chemical composition	Density, kg/l	Color	Working temperature. °C	pH
Sika Ferrogard 901	2-dimethyl tetra amino ethanol	1.06	green	1-35	10

Table 3. *Chemical composition of reinforcements*

	C (max.)	S (max.)	P (max.)	Si (max.)	Mn (max.)	Ni	Cr	Mo
	Content, %							
AISI 304	0.08	0.03	0.045	1	2	8-10.5	18-20	-
A-20	0.18-0.21	0.03	-	-	-	-	-	-

Table 4. *Amounts of used materials in mixing designs*

Concrete mixing design	Curing time, day	Amount of used materials, kg m^{-3}							
		Cement	Water	MS	FA	Sand	Crushed stone	Inhibitor	SP[1]
A	28	400	160	-	-	736	1064		1
B	28	400	160	-	-	736	1064	12	
C	28	400	216	0	100	736	1064		1.35

[1]Superplasticiser (SP) was used 0.25 % by weight of binder (cement+FA+MS).

Sample preparation

Reinforcement preparation

Steel rebar with 10 mm of diameter was cut to 120 mm of length and so to intensify acid pickling and degreasing, reinforcements were ultrasonically cleaned in a 15 % HCl solution with 0.005 % urotropin (as a corrosion inhibitor) for 20 min and in acetone for 3 min, respectively.

Concrete molding

Concrete samples with 10×10×10 cm dimensions were prepared according to BS 1881 Part 116 standards [41] to perform compression strength tests. Samples of corrosion experiments with a cylindrical shape were prepared exactly such that the reinforcement with 10 mm diameter is centrally embedded (as shown in Figure 1).

To seal the reinforcement, Teflon tape was utilized, and epoxy paint was used over it. The effective surface of the reinforcement in concrete was chosen to be 18.85 cm^2 ($S = 2\pi rh$, where r = 5 mm and h = 60 mm). Concrete samples after 24 hours were brought out of the 120 mm height molds and were placed in the curing room at a relative humidity of 90±5 for 28 days to complete the hydration reaction. The outer surface of the concrete was covered with a 2 mm height wax from both sides (top and bottom) to limit the diffusion of chloride ions only in the radial direction and also prevent corrosion in the common interfaces of concrete and reinforcement and atmosphere.

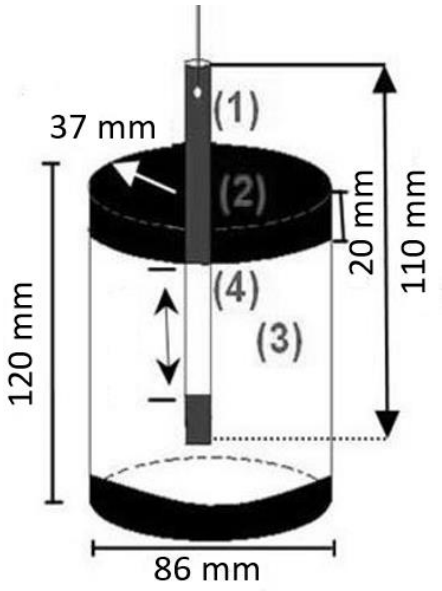

(1) Epoxy coat used for reinforcement sealing
(2) Wax used in order to concrete sealing
(3) Effective surface (18.85 cm^2)
(4) Concrete

***Figure 1**. Schematic of concrete sample for the impressed current experiment*

Reinforcement coating

To create hot dip galvanized steel (HDGS), prepared rebar was placed in the ammonium chloride flux solution for 30 seconds and subsequently was immersed in pure zinc, with 0.3 % aluminum, a melt bath at 470 °C for 2 minutes. After quenching in water, the average thickness of the galvanizing from the 3 points was reported at approximately 100±5 μm.

Impressed voltage experiment

An accelerated corrosion test under constant potential was accomplished through a DC power source, an experimental sample, and a plastic dish containing 3.5 wt.% NaCl solution, two steel plates, and a designed data logger to collect the current data of reinforced concrete every five minutes [42-46]. Indeed, a working electrode, reinforcement embedded in concrete as an anode, directly connected to the positive pole of the DC power source such that the auxiliary electrode, two stainless plates as a cathode, connected to the negative terminal, afterward a 30 V impressed voltage between the counter and the working electrode to fix stress is put on. The destruction happened when a longitudinal crack with a 0.5-1 mm width was observed in the concrete sample [47]. The impressed-voltage test setup was demonstrated in Figure 2.

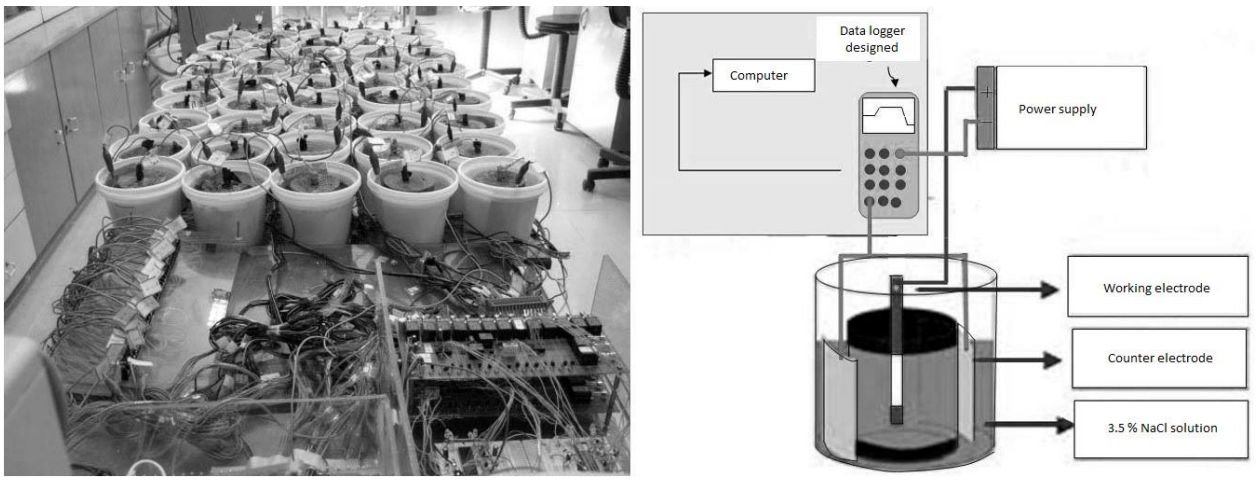

***Figure 2.** Impressed voltage experiment setup for accelerating of steel corrosion in concrete*

Fundamentals of intelligent systems

ANNs structure

Artificial neural networks (ANNs) are mathematic algorithms based on the behavior of human brain abilities and belong to dynamic systems which, by processing on the experimental data, transfer hidden knowledge or rule behind the data to the network structure. Then the neural network on the basis of acquired knowledge, can respond to a set of new data [47] and maintain a good connection between nonlinear data relations [34].

To accomplish a safe artificial neural network modeling, the following steps must be precisely defined [49]. These stages concern data gathering, defining input variables, analyzing, and pre-processing data, creating a network architecture, training the network, testing the trained network, and using the trained network for calculation and prediction. Indeed, in designing the network architecture step, the number of hidden layers, the number of neurons in the hidden layers, and the transfer function type in the hidden layer must be created. No rule exists to determine the optimum amount of parameters for designing network, and they must be obtained via trial and error [50]. In the network training step, an algorithm undergoes the trend in which the matrix of connection weights and network bias vectors are adjusted. Briefly, the training procedure is as follows: initial biases and connection weights are estimated, then with the output results of the network, initial biases and connection weights are modified so that it converges to real output results. This modification continues until the error reaches the desired value. The more the network is trained the more the error trend in each epoch tends to zero and when the error parameter reaches its minimum value, the training operation stops [37,49]. However, a low error is not always a good indicator of a better network. Cross-validation is a highly recommended criterion to stop network training [51]. The training algorithm is shown in the flow chart of Figure 3 [52].

Among different ANN architectures, the backpropagation learning algorithm is one of the simplest methods and has a more applicable learning algorithm, and is closer to human task behavior, such as predicting and categorizing. ANNs can be designed in different ways. One of the most popular ones is Multilayer's feed-forward neural networks [48,51].

This method is slow learning and needs more iterations before convergence. To obtain a performance index, a bellow performance index can be used. Predicted and experimental values are compared with the root mean square error (RSME), the mean absolute percentage error (MAPE), and the correlation coefficient (R). RSME, MAPE and R are calculated by the equations (1) to (3):

$$\mathrm{RMSE} = \sqrt{\frac{1}{p}\sum\left|t_\mathrm{i} - o_\mathrm{i}\right|^2} \tag{1}$$

$$\mathrm{MAPE} = \left|\frac{t_\mathrm{i} - o_\mathrm{i}}{o_\mathrm{i}}\right| 100 \tag{2}$$

$$R = \sqrt{1 - \left(\frac{\sum\left|t_\mathrm{i} - o_\mathrm{i}\right|^2}{\sum\left|o_\mathrm{i}\right|^2}\right)} \tag{3}$$

where t_i is the experimental values, o_i is the predicted values, and p is the number of data points [50]. In this work, the feed-forward backpropagation algorithm from the MATLAB neural network toolbox is used.

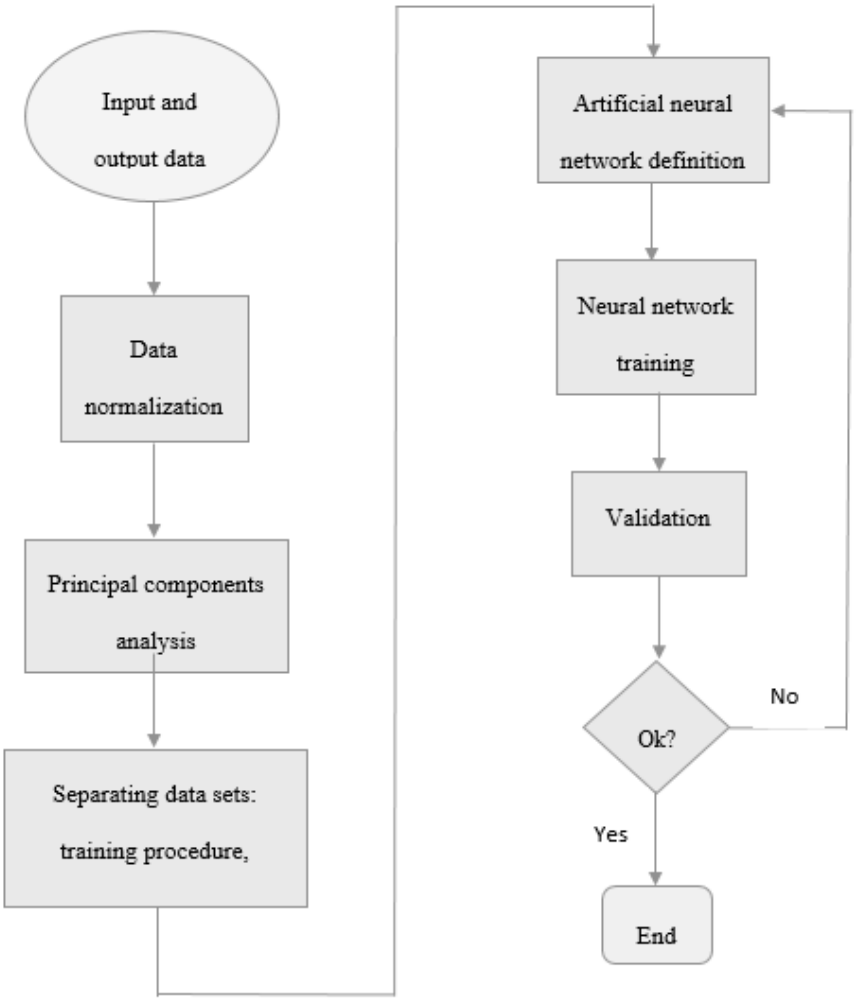

Figure 3. *Flowchart encompassing data pre-processing and ANNs training [52]*

FL background

Expert systems as technology started in the early 1950s and remained in research laboratories, and never broke through to the consumer market. FL theory which was introduced by Lotfi A. Zadeh extends conventional Boolean logic (0 and 1) [53]. The fuzzy set theory provides a means to represent uncertainty, and everything is based on a degree. So, an object can be, to some extent, a member of a set. The membership function of a fuzzy set is allowed to have values between 0 and 1, which denotes the degree of membership of an element in a given set. The continuum of logical values between 0 (completely false) and 1 (completely true) are used. In contrast to the crisp theory with a sharp boundary, the fuzzy set theory has no sharp boundary. Usually, fuzzy set and membership information is illustrated by equation (4):

$$\mu_A(X) = z \quad (4)$$

This says the membership (μ) of X in fuzzy set A is z [54]. The membership function can be an arbitrary curve, but there are several common membership functions for use in engineering applications, such as piecewise linear functions, the Gaussian distribution function, the sigmoid curve, and quadratic and cubic polynomial curves, *etc.* Fuzzy inference is the process of formulating the mapping from a given input to an output using fuzzy logic. There are two types of fuzzy inference systems used extensively: the Mamdani-type and the Sugeno-type. The Sugeno or Takagi-Sugeno-Kang (TSK) method of fuzzy inference was introduced in 1985 [53,54]. The output membership function of the Sugeno-type fuzzy inference system is linear or constant. Clustering involves the task

of dividing data points into homogeneous classes or clusters so that items in the same class are as similar as possible and items in different classes are as dissimilar as possible. Subtractive clustering is a fast, one-pass algorithm to estimate the number of clusters and cluster centers in the data set [53,55]. Subtractive clustering is an effective approach to estimating the number of fuzzy clusters and cluster centers [56]. To predict the corrosion current by fuzzy logic experimental of corrosion current, the corrosion time and the concrete type are loaded in the MATLAB fuzzy logic tool, and the corrosion current model is constructed. Detailed steps of the corrosion current model construction with fuzzy logic are described next.

Results and discussion

Compressive strength and corrosion analysis in concrete

The results of the compressive strength experiment and the cracking initiation time of three mix proportions are depicted in Table 5. According to the outcomes, the compressive strength of mix design C, the pozzolanic concrete, compared with the control concrete, mix proportion A, is decreased from 57.64 to 54.29 MPa, while the usage of corrosion inhibitor admixture, mix proportion C, suggests less decreasing of the compressive strength of concrete. It is worth mentioning that a similar decrement in concrete strength is also shown elsewhere [57,58]. Indeed, completing the hydration reaction of pozzolanic materials is a time-consuming process and mainly using the pozzolanic component can delay the process [57]. However, seeing a porosity decrement, they are expected to increase the corrosion resistance of steel reinforcement in the concrete [59].

Table 5. *Compressive strengths and damage occurrence times*

Mix proportion		A		B	C
Reinforcement type	A-20	AISI-304	HDGS	A-20	A-20
Cracking initiation time, h	26	56	38	154	183
Concrete compressive strength, MPa		57.64		56.12	54.29

In accordance with Table 5, due to rebar corrosion in control, concrete destruction only can take place after 26 hours after applying a constant anodic voltage of 30 V. Furthermore, corrosion initiation came about when the passive and protective surface layer on the reinforcement was broken, and the corrosion progression continued with high velocity through the environment to the reinforcement surface. Basically, the formation of the corrosion products and subsequently the volume enhancement of corrosion layers approaching the reinforcement can be imposed a high degree of internal stress equal to 450 MPa to concrete and eventually bring about the failure of the concrete [44,60]. Concrete failure is shown in Figure 4.

In the mixed designs of B and C, which were introduced as protection methods, the failure time of concrete was increased to 154 and 183 hours, respectively. It is important to mention that in this condition, a reinforcement type of A-20 grade was selected and only the effect of the concrete additive needs to be explained. Fundamentally, the effect of the pozzolanic materials to improve the corrosion resistance of steel in concrete can be explained by the effective role of the pozzolanic component in closing or decreasing concrete porosity [61]. Equivalently, Ferrogard 901 corrosion inhibitor admixture, through its reaction with the free chloride ions and the decrement of their concentration over the rebar surface, reduces the corrosion product amount in reinforcement concrete [62].

Figure 4. *Destruction of concrete samples after accelerated corrosion test*

The influence of changing the rebar type concerning HDGS and AISI-304 was evaluated at mix design A. Outcomes directly extracted from Table 3 obviously illustrate using HDGS and AISI-304 as an alternative to A-20 rebar can improve the destruction time to 38 and 41 hours, respectively. Although stainless AISI-304 is more sustainable to pitting corrosion regarding chloride ions and easily broken the passivation film, some corrosion-resistant elements, such as Ni, Cr and Mn, postpone corrosion advancement and, as a result, crack propagation can be delayed [63,64].

Zinc coated steel rebar or HDGS shows approximately 38 hours of failure resistance to 30V impressed voltage in the NaCl solution, which is clearly more than ordinary steel and less than stainless steel AISI-304. Mainly Zn element appears as a sacrificial anode and, with consumption during the electrochemical reaction, likely protects the steel from corrosive ions [65,66].

NN structure design and its parameters

This study attempts to simulate the effect of time duration on steel corrosion in the concrete mix design, then evaluates the addition of pozzolanic materials type to concrete in the second model, and eventually compare the results with other proposed protection methods at the third network, *i.e.,* as mentioned earlier changing the reinforcement type, coating, and influence of corrosion inhibitor.

Three models are discussed so that in the first network, the interval time imported as an input parameter and the galvanic corrosion current under a rapid chloride diffusion experiment acted as an output result in which one hidden layer with ten neurons and a log-sig transfer function has been used. Figure 5 schematically represents the first neural network architecture.

The second model is designed to simulate the pozzolanic additive in concrete. Built ANNs structure in the first simulation was used to predict the missing corrosion current in the second simulation. This model is more general to predict corrosion current on the basis of more inputs, such as cement type, *i.e.,* cement type II, FA and MS, and corrosion time. Thus, in this model, ANNs have 2 inputs and one output, and the built structure consists of one hidden layer with 10 neurons and a log-sig transfer function observed in Figure 6. About 356 data points were obtained from experiments and 75 % of them were used for training and the remaining were used for testing and network validation.

In the third prediction, the influence of changing reinforcement type, reinforcement coating, and the corrosion inhibitor admixture were verified, and in each case, the corrosion current was measured. In this model, ANNs have 4 inputs and one output and the built structure consists of one hidden layer with 20 neurons and the tan-sign transfer function, which can be observed in Figure 7.

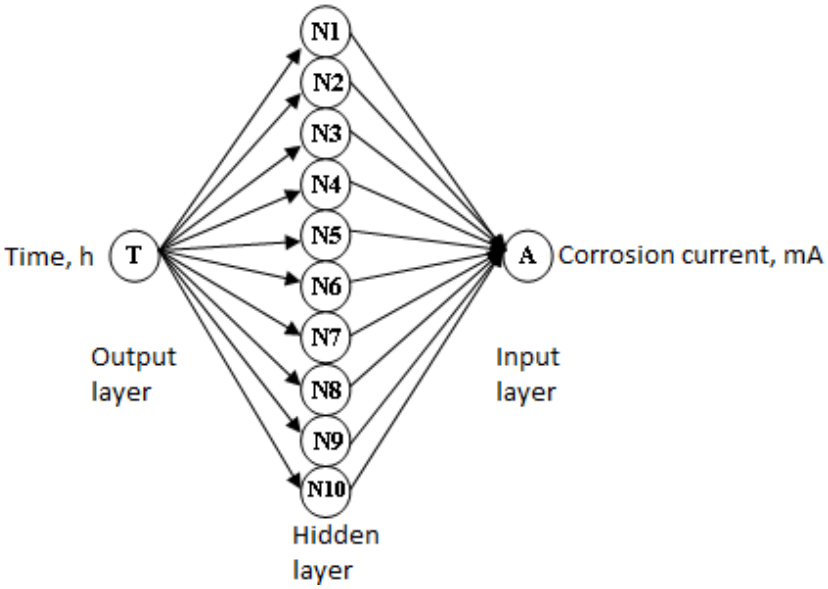

***Figure 5**. Used system in the ANNs model for the first simulation*

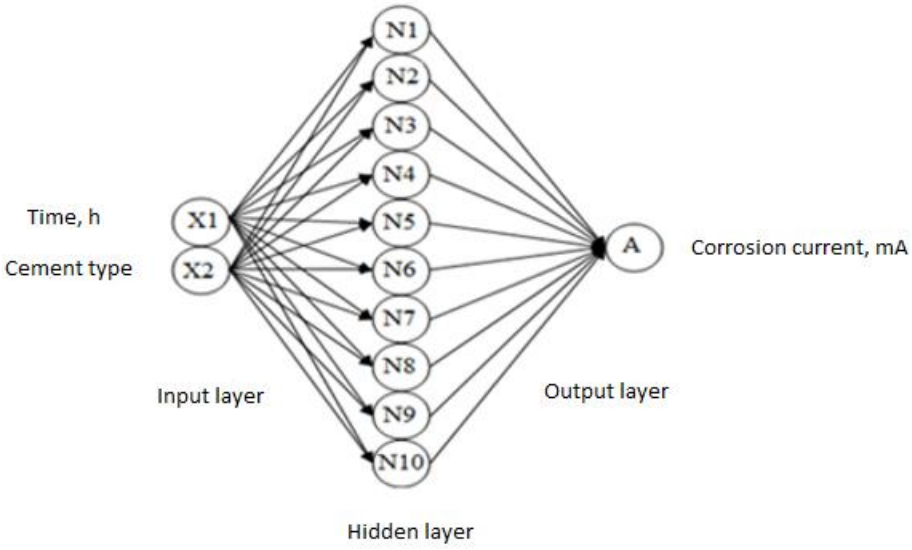

***Figure 6.** Used system in the ANNs model for the second simulation*

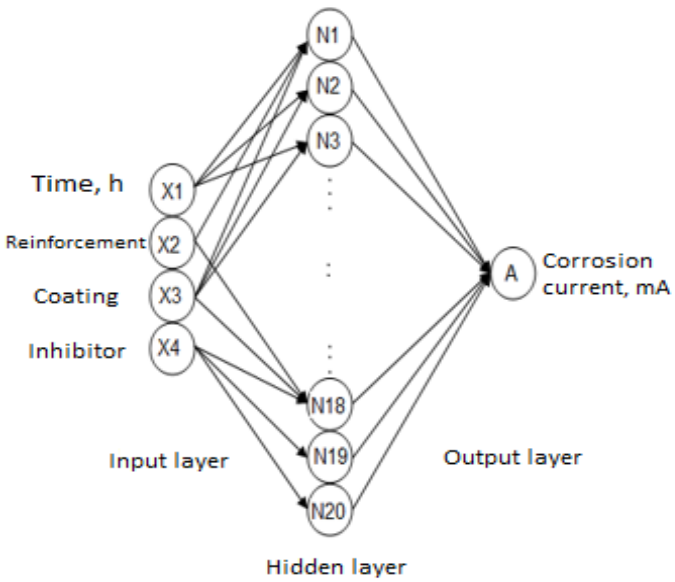

***Figure 7.** Proposed architecture to simulate the third part*

About 2492 data points were obtained from experiments and 75 % of them were used for training and the remaining were used for testing and network validation. Regarding the log-sig transfer function, the upper and lower limits of the network input and output must be between zero to one, so input and output data must be normalized. After network training, it must be tested.

Corrosion behavior analysis by ANNs

All parameters in the three described simulations are summarized in Table 6. Indeed, results obtained by performance and error indicators were represented in Table 6.

Table 6. *Performances of ANNs to predict the galvanic corrosion current*

Parameters				$R_{training}$	$R_{testing}$	$R_{validation}$	R_{total}	MSE	MAPE
Simulation	(I) Corrosion time	Mix design	A	0.99799	0.9952	0.99284	0.99648	4.9578	0.0520
			B	0.99788	0.99699	0.99682	0.99632	4.5632	0.1101
			C	0.99517	0.99861	0.99845	0.99654	4.0097	0.1600
	(II) Cement type			0.99546	0.99641	0.99709	0.99595	7.9966	1.4789
	(III) Protection methods			0.99011	0.98476	0.99216	0.98933	5.4654	0.5834

According to performance and error indicators, it can be stated that the ANN model provides a precise answer for the corrosion current simulation. As an example, in case C in Table 6, the simulation regression coefficient is R = 0.99654. Since $0 \le R \le 1$, the higher R represents a better match between the predicted corrosion current and the experimental corrosion current [67]. A typical result of the predicted corrosion current data and the experimental corrosion current data versus the corrosion time in mix design C according to the first simulation model are shown in Figure 8.

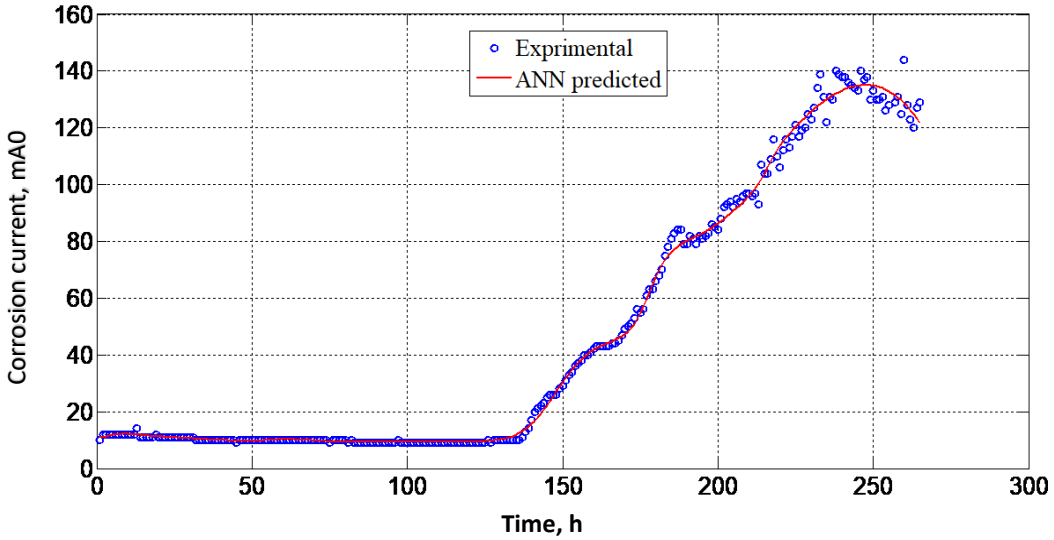

Figure 8*. Experimental and predicted corrosion current by ANN versus time for first simulation (mix design C)*

Also, the results of the predicted corrosion current data versus the experimental corrosion current data for simulations I and III are typically shown in Figure 9. The distribution between the predicted values and the experimental values has been modeled by the linear approach and its best linear equation was obtained. This equation is also shown in Figure 9.

It can be observed in Figures 8 and 9 that trained ANNs structure in the nonlinear deviated regions predicts a successful and precise response. Also, to demonstrate the precision of the proposed models, an error criterion as the difference between the predicted and experimental data versus time is suggested in Figure 10, which illustrates the high precision of the modeled network.

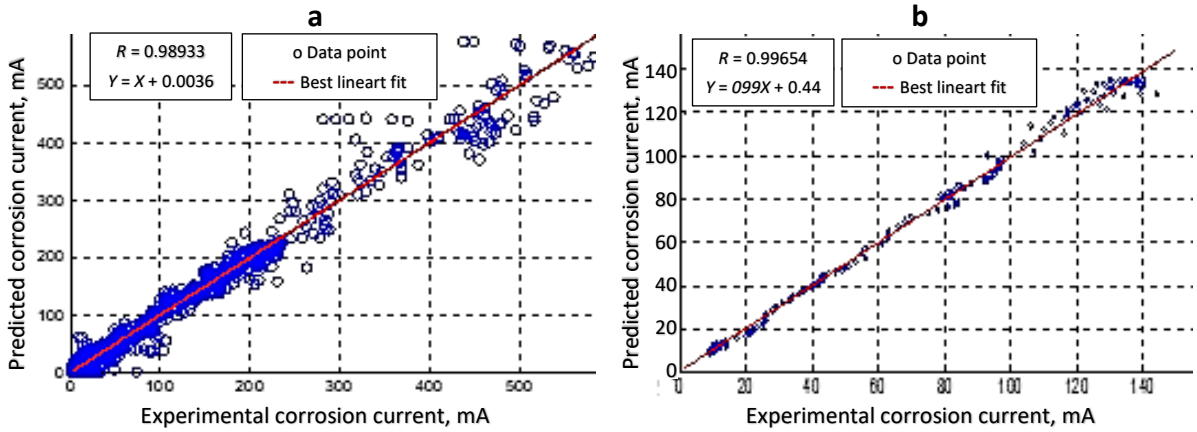

Figure 9. *Typical predicted data versus experimental corrosion currents by ANN, also best linear fit, (a) first and (b) third simulation*

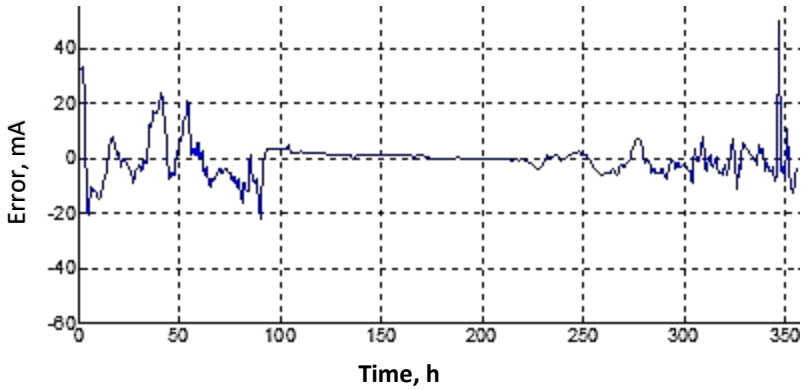

Figure 10*. Typical error of corrosion versus time of corrosion by ANNs for the second simulation*

Fuzzy logic results

Similar to the earlier simulation, neural network data of each corrosion setup were combined, and a comprehensive data set was formed. Data were grouped into two sets: training data (75 % of data) and testing data (25 % of data), which were randomly selected. Training data were used to generate and train a sugeno-type FIS and testing data were used to validate and verify the model. By extracting membership functions and fuzzy if-then rules, the Takagi-Sugeno fuzzy model was constructed. A comparison between predicted and experimental corrosion current results was made with the same performance and error indicators used in the ANN simulation. The results of the trained network performance and error indicators are shown in Table 7.

Table 7. *Performances of the fuzzy logic built*

	Parameter		MSE	MAPE	*R*
Simulation	(I) Corrosion time	Training	4.2166	0.9729	0.9992
		Testing	5.2223	0.5394	0.9991
	(II) Cement type	Training	3.9966	1.3245	0.9993
		Testing	4.5646	1.1974	0.9934
	(III) Protection methods	Training	1.0197	1.4799	0.9938
		Testing	2.0200	1.2990	0.9937

Results of the trained network performance and error indicators show the good accuracy of the fuzzy logic. Also, to show the results and network performance predicted corrosion current versus the values of experimental corrosion current in training and testing is shown in Figure 11.

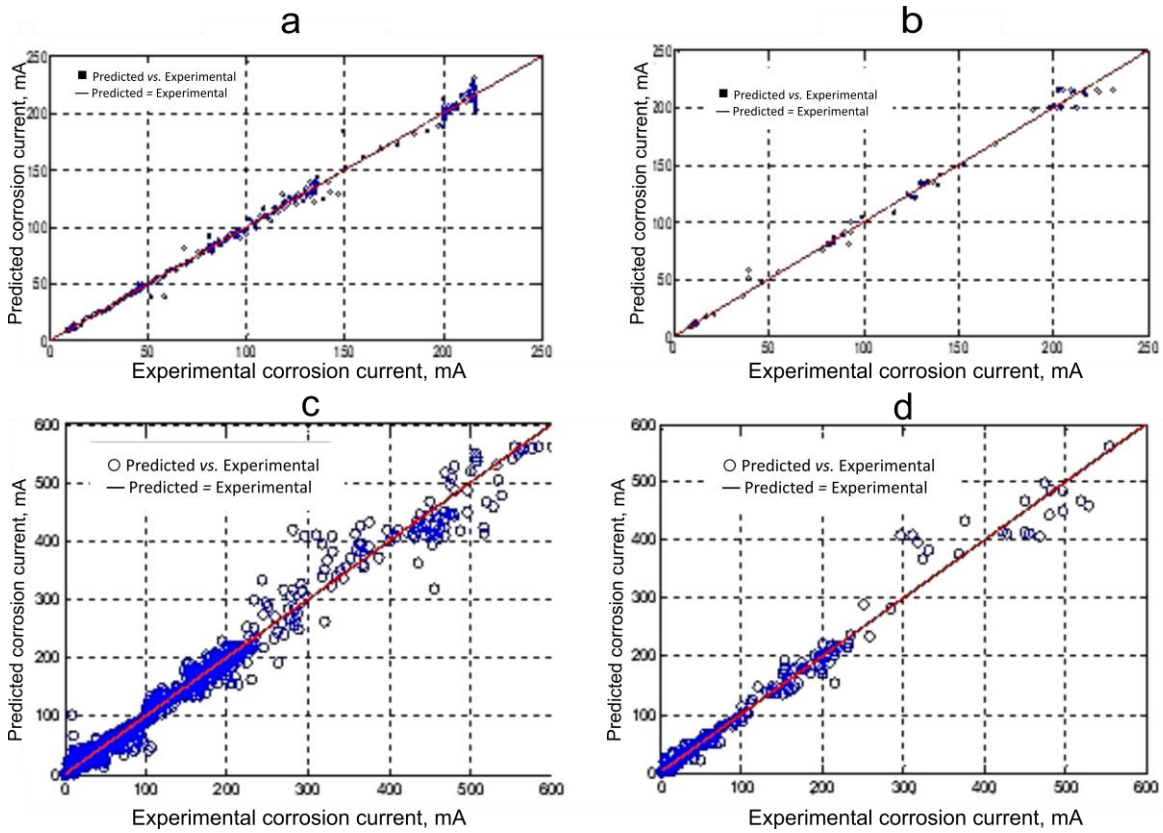

Figure 11. *Typical predicted data versus experimental corrosion currents of fuzzy logic model: (a), (b) training and testing for the first model (c), (d) training and testing for the third model*

To show model precision, an error criterion, as the difference between predicted data and experimental data versus time, is shown in Figure 12, which confirms the successfulness and high precision of the modeled network.

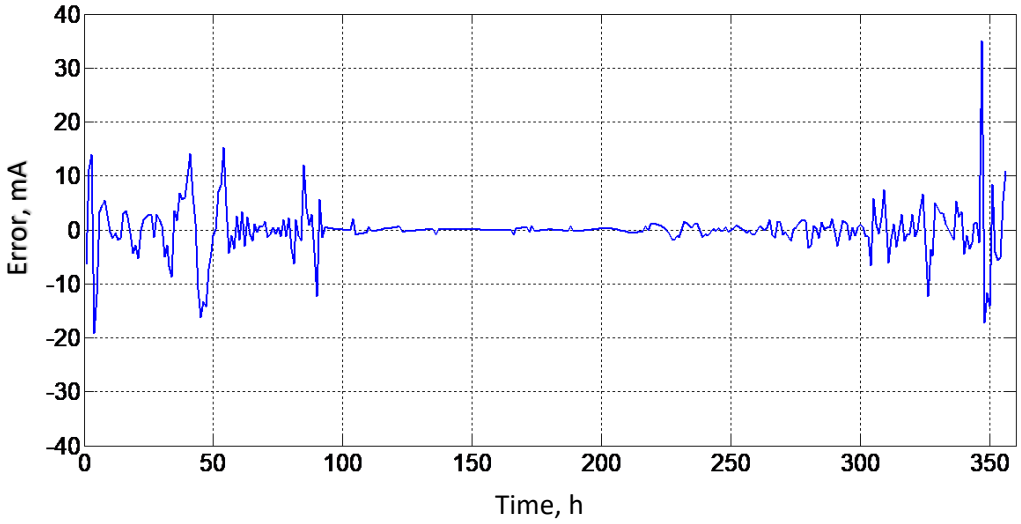

Figure 12. *Error of corrosion versus time of fuzzy logic model*

The contribution factor (CF) measures the importance of the respective parameter in predicting the network's output relative to other network input parameters. The higher the absolute sum of those weights is, the more the parameter contributes to classification. However, neural networks can also find patterns among several parameters, none of which is highly correlated with output, but which together form a pattern that uniquely determines the output [68]. The CF for individual input parameters in predicting the corrosion current was evaluated in Figure 13.

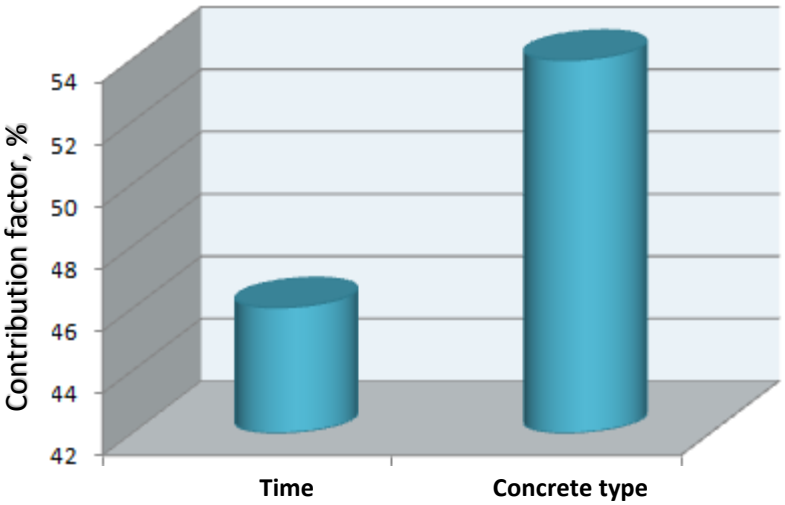

Figure 13. *Contribution factor for individual input parameters in predicting the damage of reinforcement concrete*

The CF predicts which model more effectively reduces corrosion damage. Clearly, Figure 13 demonstrates the effect of corrosion protective methods, such as the addition of FA and MS in the preferred percent to mix design, altering the reinforcement type, coating steel by the zinc element or the galvanizing method and corrosion inhibitor admixture to concrete. Undoubtedly, all options besides interval time are so important in selecting the best state, but as described, the contribution of each approach to decrease corrosion here is important. Predictions show using FA and MS as pozzolanic materials with a CF of approximately 35 % is the most important parameter to reduce steel corrosion in concrete. After that, controlling the elapsed time from construction is crucial. In other protective ways, utilizing the corrosion inhibitor, changing reinforcement with AISI-304, and coating the reinforcement with galvanizing are the next options

Using ANNs and FL in special concretes like reinforced self-compacting concrete (SCC), including nano-clay particles and coated rebars (polyurethane and alkyd top coating) is an area that needs to be studied in the future. There are various publications in the supercapacitor in terms of energy density, different materials, microstructures, output current density, life cycle, *etc.* However, utilizing the ANNs and FL methods to predict the effects of the aforementioned parameters on the efficiency of supercapacitor and its practicality has not been studied yet, and it would be a great area to implement these methods [69-73].

Conclusion

Steel corrosion in concrete is a complicated process that can be predicted through powerful artificial intelligence tools, such as ANNs and FL. In this study, the influence of different protection methods to enhance the corrosion resistance of reinforced concrete as addition of FA and MS in the preferred content to concrete, approximately 25 and 10 wt.% cement respectively, replacement stainless steel (AISI-304) with carbon steel, the coating of rebar by the hot dip galvanizing method, and the usage of Ferrogard 901 to concrete mixing design, were analyzed and corrosion current results were simulated by ANNs and FL. The ANN and FL are responsive even when the corrosion current shows deviational and nonlinear behavior. It can be concluded that ANNs and FL could be appropriate techniques to model the corrosion current of rebar in concrete. Predictions from the three designed networks show the utilization of FA and MS as pozzolanic materials with a CF of approximately 35 % is the most important parameter to reduce steel corrosion in concrete.

References

[1] A. Afshar, S. Jahandari, H. Rasekh, M. Shariati, A. Afshar, A. Shokrgozar, *Construction and Building Materials* **262** (2020) 120034. https://doi.org/10.1016/j.conbuildmat.2020.120034

[2] M. Saberian, S. Jahandari, J. Li, F. Zivari, *Journal of Rock Mechanics and Geotechnical Engineering* **9(4)** (2017) 638-641. https://doi.org/10.1016/j.jrmge.2017.01.004

[3] S. Jahandari, M. Saberian, Z. Tao, S. F. Mojtahedi, J. Li, M. Ghasemi, S. S. Rezvani, W. Li, *Cold Regions Science and Technology* **160** (2019) 242-251. https://doi.org/10.1016/j.coldregions.2019.02.011

[4] S. Jahandari, M. M. Toufigh, J. Li, M. Saberian, *Geotechnical and Geological Engineering* **36** (2018) 413-424. https://doi.org/10.1007/s10706-017-0335-4

[5] F. Sadeghian, A. Haddad, S. Jahandari, H. Rasekh, T. Ozbakkaloglu, *Canadian Geotechnical Journal* **58(5)** (2021). https://doi.org/10.1139/cgj-2019-0650

[6] H. Rasekh, A. Joshaghani, S. Jahandari, F. Aslani, M. Ghodrat, *Self-Compacting Concrete: Materials, Properties and Applications,* Woodhead Publishing Series in Civil and Structural Engineering, London, United Kingdom (2020) 31-63. https://doi.org/10.1016/B978-0-12-817369-5.00002-7

[7] S. Jahandari, S. F. Mojtahedi, F. Zivari, M. Jafari, M. R. Mahmoudi, A. Shokrgozar, S. Kharazmi, B. Vosough Hosseini, S. Rezvani, H. Jalalifar, *Geomechanics and Geoengineering* **17(1)** (2020) 269-281. https://doi.org/10.1080/17486025.2020.1739753

[8] A. Toghroli, P. Mehrabi, M. Shariati, N. T. Trung, S. Jahandari, H. Rasekh, *Construction and Building Materials* **252** (2020) 118997. https://doi.org/10.1016/j.conbuildmat.2020.118997

[9] M. Kazemi, M. Hajforoush, P. K. Talebi, M. Daneshfar, A. Shokrgozar, S. Jahandari, M. Saberian, J. Li, *Journal of Sustainable Cement-Based Materials* **9(5)** (2020) 289-306. https://doi.org/10.1080/21650373.2020.1734983

[10] M. Rezania, H. Moradnezhad, M. Panahandeh, M. J. R. Kami, A. Rahmani, B. V. Hosseini, *Journal of Building Engineering* **31** (2020) 101343. https://doi.org/10.1016/j.jobe.2020.101343

[11] M. Kazemi, J. Li, S.L. Harehdasht, N. Yousefieh, S. Jahandari, M. Saberian, *Structures* **23** (2020) 87-102. https://doi.org/10.1016/j.istruc.2019.10.013

[12] L. Bertolini, B. Elsener, P. Pedeferri, E. Redaelli, R. B. Polder, *Corrosion of Steel in Concrete: Prevention, Diagnosis, Repair,* John Wiley & Sons, 2013. ISBN: 978-3-527-33146-8

[13] B. Elsener, *Materials Science and Technology,* Wiley-VCH Verlag GmbH & Co. KGaA, 2006.

[14] M. El-Reddy, *Steel Reinforced Concrete Structures: Assessment and Repair of Corrosion,*. CRC Press, New York, 2007. ISBN 9781138066984

[15] C. L. Page, J. Havdahl, *Materials and Structures* **18** (1985) 41-47. https://doi.org/10.1007/BF02473363

[16] O. Kayali, *Construction and Building Materials* **22(12)** (2008) 2393-2399. https://doi.org/10.1016/j.conbuildmat.2007.09.001

[17] A. L. A. Fraay, J. M. Bijen, Y. M. de Haan, *Cement and Concrete Research* **19(2)** (1989) 235-246. https://doi.org/10.1016/0008-8846(89)90088-4

[18] W. Aperador, R. Mejía de Gutiérrez, D. M. Bastidas, *Corrosion Science* **51(9)** (2009) 2027-2033. https://doi.org/10.1016/j.corsci.2009.05.033

[19] D. D. N. Singh, S. Yadav, *Surface and Coatings Technology* **202(8)** (2008) 1526-1542. https://doi.org/10.1016/j.surfcoat.2007.07.013

[20] D. D. N. Singh, R. Ghosh, *Surface and Coatings Technology* **202(19)** (2008) 4687-4701. https://doi.org/10.1016/j.surfcoat.2008.03.038

[21] M. M. Al-Zahrani, S. U. Al-Dulaijan, M. Ibrahim, H. Saricimen, F. M. Sharif, *Cement and Concrete Composites* **24(1)** (2002) 127-137. https://doi.org/10.1016/S0958-9465(01)00033-6

[22] A. Bautista, A. González-Centeno, G. Blanco, S. Guzmán, *Materials Characterization* **59(1)** (2008) 32-39. https://doi.org/10.1016/j.matchar.2006.10.008
[23] W. Morris, M. Vázquez, *Cement and Concrete Research* **32(2)** (2002) 259-267. https://doi.org/10.1016/S0008-8846(01)00669-X
[24] S. Akkurt, G. Tayfur, S. Can, *Cement and Concrete Research* **34(8**) (2004) 1429-1433. https://doi.org/10.1016/j.cemconres.2004.01.020
[25] F. Özcan, C.D. Atiş, O. Karahan, E. Uncuoğlu, H. Tanyildizi, *Advances in Engineering Software* **40(9)** (2009) 856-863. https://doi.org/10.1016/j.advengsoft.2009.01.005
[26] M. Sarıdemir, I. B. Topçu, F. Özcan, M. H. Severcan, *Construction and Building Materials* **23(3)** (2009) 1279-1286. https://doi.org/10.1016/j.conbuildmat.2008.07.021
[27] M. Sarıdemir, *Advances in Engineering Software* **40(9)** (2009) 920-927. https://doi.org/10.1016/j.advengsoft.2008.12.008
[28] H. Tanyildizi, *Advances in Engineering Software* **40(3)** (2009) 161-169. https://doi.org/10.1016/j.advengsoft.2007.05.013
[29] I. B. Topçu, C. Karakurt, M. Sarıdemir, *Materials & Design* **29(10)** (2008) 1986-1991. https://doi.org/10.1016/j.matdes.2008.04.005
[30] I. B. Topçu, M. Sarıdemir, *Computational Materials Science* **41(3)** (2008) 305-311. https://doi.org/10.1016/j.commatsci.2007.04.009
[31] I. B. Topçu, M. Sarıdemir, *Computational Materials Science* **42(1)** (2008) 74-82. https://doi.org/10.1016/j.commatsci.2007.06.011
[32] I.-C. Yeh, *Cement and Concrete Research* **28(12)** (1998) 1797-1808. https://doi.org/10.1016/S0008-8846(98)00165-3
[33] I. B. Topçu, M. Sarıdemir, *Construction and Building Materials* **22(4)** (2008) 532-540. https://doi.org/10.1016/j.conbuildmat.2006.11.007
[34] I. B. Topçu, A. R. Boğa, F. O. Hocaoğlu, *Automation in Construction* **18(2)** (2009) 145-152. https://doi.org/10.1016/j.autcon.2008.07.004
[35] N. Ukrainczyk, V. Ukrainczyk, *Magazine of Concrete Research* **60(7)** (2008) 475-486. https://doi.org/10.1680/macr.2007.00016
[36] T. Parthiban, R. Ravi, G.T. Parthiban, S. Srinivasan, K. R. Ramakrishnan, M. Raghavan, *Corrosion Science* **47(7)** (2005) 1625-1642. https://doi.org/10.1016/j.corsci.2004.08.011
[37] D. M. Roy, P. Arjunan, M. R. Silsbee, *Cement and Concrete Research* **31(12)** (2001) 1809-1813. https://doi.org/10.1016/S0008-8846(01)00548-8
[38] P. S. Mangat, B. T. Molloy, *Cement and Concrete Research* **21(5)** (1991) 819-834. https://doi.org/10.1016/0008-8846(91)90177-J
[39] G. Yang, L. Ying, L. Haichao, Corrosion Science 43(3) (2001) 397-411. https://doi.org/10.1016/S0010-938X(00)00090-1
[40] A. Afshar, A. Nobakhti, A. Shokrgozar, A. Afshar, *Revista Romana de Materiale/Romanian Journal of Materials* **49(4)** (2019) 535-543. https://solacolu.chim.upb.ro/pg535-543.pdf
[41] BS 1881 116 1983 Testing Concrete. *Method for Determination of Compressive Strength of Concrete Cubes*, British Standards Institute, London, United Kingdom, 1983. https://pdfcoffee.com/bs-1881-part-116-concrete-cubes-pdf-free.html
[42] A. R. Boğa, Ý.B. Topçu, M. Öztürk, *Materiali in Tehnologije/Materials and Technology* **46(5)** (2012) http://mit.imt.si/izvodi/mit125/boga.pdf
[43] E. Güneyisi, M. Gesoğlu, *Materials and Structures* **41** (2008) 479-493. https://doi.org/10.1617/s11527-007-9260-y
[44] E. Güneyisi, T. Özturan, M. Gesoğlu, *Cement and Concrete Composites* **27(4)** (2005) 449-461. https://doi.org/10.1016/j.cemconcomp.2004.05.006
[45] V. Horsakulthai, K. Paopongpaiboon, *American Journal of Applied Sciences* **10(3)** (2013) 239-246. https://doi.org/10.3844/ajassp.2013.239.246

[46] V. Saraswathya, H.-W. Song, *Portugaliae Electrochimica Acta* **26(5)** (2008) 417-432. http://dx.doi.org/10.4152/pea.200805417
[47] K. Sakr, *Cement and Concrete Research* **35(9)** (2005) 1820-1826. https://doi.org/10.1016/j.cemconres.2004.10.015
[48] R. C. C. Silva, J. N. C. Guerreiro, A. F. D. Loula, *Advances in Engineering Software* **38(11-12)** (2007) 868-875. https://doi.org/10.1016/j.advengsoft.2006.08.047
[49] V. Kappatos, A. N. Chamos, S. G. Pantelakis, *Materials & Design* **31(1)** (2010) 336-342. https://doi.org/10.1016/j.matdes.2009.06.009
[50] B. Kröse, P. van der Smagt, *An Introduction Neural Networks*, Academic Press, New York, 1996. https://www.infor.uva.es/~teodoro/neuro-intro.pdf
[51] D. Ok, Y. Pu, A. Incecik, *Ocean Engineering* **34(17-18)** (2007) 2222-2230. https://doi.org/10.1016/j.oceaneng.2007.06.007
[52] E. D. Kenny, R. S. C. Paredes, L. A. de Lacerda, Y. C. Sica, G. P. de Souza, J. Lázaris, *Corrosion Science* **51(10)** (2009) 2266-2278. https://doi.org/10.1016/j.corsci.2009.06.004
[53] P. Melin, O. Castillo, *Hybrid Intelligent Systems for Pattern Recognition Using Soft Computing*,Springer Berlin Heidelberg, 2005, p. 1. https://doi.org/10.1007/978-3-540-32378-5_1
[54] S. L. Chiu, *Journal of Intelligent and Fuzzy Systems* **2(3)** (1994) 267-278. http://dx.doi.org/10.3233/IFS-1994-2306
[55] L. A. Zadeh, *Synthese* **30** (1975) 407-428. https://doi.org/10.1007/BF00485052
[56] J. M. Mendel, *Proceedings of the IEEE* **83(3)** (1995) 345-377. https://doi.org/10.1109/5.364485
[57] Y.-S. Choi, J.-G. Kim, K.-M. Lee, *Corrosion Science* **48(7)** (2006) 1733-1745. https://doi.org/10.1016/j.corsci.2005.05.019
[58] D. Li, J. Shen, Y. Chen, L. Cheng, X. Wu, *Cement and Concrete Research* **30(9)** (2000) 1381-1387. https://doi.org/10.1016/S0008-8846(00)00360-4
[59] V. Saraswathy, H.-W. Song, *Electrochimica Acta* **51(22)** (2006) 4601-4611. https://doi.org/10.1016/j.electacta.2006.01.005
[60] L. K. Spainhour, I. A. Wootton, *Cement and Concrete Composites* **30(6)** (2008) 535-543. https://doi.org/10.1016/j.cemconcomp.2008.02.004
[61] A. K. Parande, B. Ramesh Babu, M. Aswin Karthik, K. K. Deepak Kumaar, N. Palaniswamy, *Construction and Building Materials* **22(3)** (2008) 127-134. https://doi.org/10.1016/j.conbuildmat.2006.10.003
[62] T. A. Söylev, M. G. Richardson, *Construction and Building Materials* **22(4)** (2008) 609-622. https://doi.org/10.1016/j.conbuildmat.2006.10.013
[63] M. C. García-Alonso, M. L. Escudero, J. M. Miranda, M. I. Vega, F. Capilla, M. J. Correia, M. Salta, A. Bennani, J. A. González, *Cement and Concrete Research* **37(10)** (2007) 1463-1471. https://doi.org/10.1016/j.cemconres.2007.06.003
[64] G. Ping, S. Elliott, J. J. Beaudoin, B. Arsenault, *Cement and Concrete Research* **26(8)** (1996) 1151-1156. https://doi.org/10.1016/0008-8846(96)00110-X
[65] T. Bellezze, M. Malavolta, A. Quaranta, N. Ruffini, G. Roventi, *Cement and Concrete Composites* **28(3)** (2006) 246-255. https://doi.org/10.1016/j.cemconcomp.2006.01.011
[66] Z. Q. Tan, C. M. Hansson, *Corrosion Science* **50(9)** (2008) 2512-2522. https://doi.org/10.1016/j.corsci.2008.06.035
[67] I.-C. Yeh, *Cement and Concrete Composites* **29(6)** (2007) 474-480. https://doi.org/10.1016/j.cemconcomp.2007.02.001
[68] N. Ukrainczyk, I. Banjad Pecur, N. Bolf, *Civil Engineering and Environmental Systems* **24(1)** (2007) 15-32. https://doi.org/10.1080/10286600601024749

[69] Y. A. Kumar, S. Sambasivam, S. A. Hira, K. Zeb, W. Uddin, T. N. V. Krishna, K. D. Kumar, I. M. Obaidat, H.-j. Kim, *Electrochimica Acta* **364** (2020) 137318. https://doi.org/10.1016/j.electacta.2020.137318
[70] R. Ahmad, N. Iqbal, M. M. Baig, T. Noor, G. Ali, I. H. Gul, *Electrochimica Acta* **364** (2020) 137147. https://doi.org/10.1016/j.electacta.2020.137147
[71] A. M. Sampaio, G. F. L. Pereira, M. Salanne, L.J. A. Siqueira, *Electrochimica Acta* **364** (2020) 137181 https://doi.org/10.1016/j.electacta.2020.137181
[72] A. R. Mule, S. K. Hussain, B. N. V. Krishna, J. S. Yu, *Electrochimica Acta* **364** (2020) 137231. https://doi.org/10.1016/j.electacta.2020.137231
[73] S. Liu, S. Sarwar, H. Zhang, Q. Guo, J. Luo, X. Zhang, *Electrochimica Acta* **364** (2020) 137320. https://doi.org/10.1016/j.electacta.2020.137320